Ahmadi, Mohammad Mahdi; Ayyoubzadeh, Seyed Ali; Namin, Masoud Montazeri; Samani, Jamal Mohammad Vali

Depth Averaged Two-Dimensional Numerical Modeling of Unsteady Flow in Open Channel Bends

Depth Averaged Two-Dimensional Numerical Modeling of Unsteady Flow in Open Channel Bends

M. M. Ahmadi[1], S. A. Ayyoubzadeh[2], M. Montazeri Namin[3] and J. M. V. Samani[4]

[1] Associate Professor , Department of Hydraulic Structures, College of Agriculture, Tarbiat Modarres University, Tehran, Islamic Republic of Iran, e-mail: ahmadi_me17@yahoo.com
[2] Associate Professor ,Department of Hydraulic Structures, College of Agriculture, Tarbiat Modarres University, Tehran, Islamic Republic of Iran, e-mail: Ayyoubzade@yahoo.com
[3] Associate Professor ,Department of Civil Engineering, Tehran University, Tehran, Islamic Republic of Iran, e-mail: Namin@yahoo.com
[4] Associate Professor ,Department of Hydraulic Structures, College of Agriculture, Tarbiat Modarres University, Tehran, Islamic Republic of Iran.

ABSTRACT

The purpose of this paper is to present a 2D depth-average model for simulating and examining unsteady flow patterns in open channel bends. In particular, this paper proposes a 2D depth-averaged model that takes into account the influence of secondary flow phenomenon through the calculation of the dispersion stresses. The dispersion terms arisen from the integration of the product the discrepancy between the mean and the actual vertical velocity distribution were included in the momentum equations to take into account the effect of secondary current. This model used time-splitting method for solving advection, diffusion and other momentum equations terms. The proposed model uses an orthogonal curvilinear coordinate system to efficiently and accurately simulate the flow field with irregular boundaries and used finite volume projection method approach for solving the governing equation in a staggered grid. Two sets of experimental data were used to demonstrate the model capabilities. The comparison of the simulated velocity and water surface elevation with the measurements shows good agreement and indicates that the inclusion of the dispersion terms has improved the simulation results.

Keywords: Unsteady flow, Open channels, two dimensional model, Numerical models, Meander, bend.

1. INTRODUCTION

Flow characteristics in meandering channels are much more complicated than those in straight reaches. Due to the secondary flow, flow passing through meandering channel is of a three-dimensional nature.

Secondary flow results from the imbalance between the transverse water surface gradient force and centrifugal force over the depth due to the vertical variation of the primary flow velocity. In other word, the inward pressure gradient near the bed prevails over the centrifugal force resulting in an inward flow along the bed and outward flow near the water surface.

Pioneering investigation of the flow phenomena in open channel bends are generally attributed to Thompson (1876) who observed the spiral motion inherent in a channel bend by introducing seeds and dyes into the flow. Since then, many studies have been conducted on flows in bends [e.g., Mockmore (1943), Shukhry (1949), Rozovskii (1961), and Yen (1965)].

To accurately simulate flow in meandering channels, flow passing through meandering channels requires a 3D hydrodynamic model. Many 3D numerical models have been developed (Leschziner and Rodi, 1979; Sinha et al. 1998; Wu et al. 2000; Meselhe and Sotiropoulos 2000) to simulate the complicated spiral flow motion in river bends. When dealing with the practical engineering problems, such as alluvial geomorphic processes, it is not computationally efficient to use 3D models. Instead, researchers (Howard 1984; Smith 1984; Johannesson and Parker 1989a, b; Nelson and Smith 1989; Odgaard 1989; Shimizu and Itakura 1989; Molls and Chaudhry 1995; Ye and McCorquodal 1997; Lien et al. 1999; Darby et al. 2002; Hsieh and Yang 2003) applied two dimensional (2D) models to simulate meandering channel flow.

The 2D depth-averaged models used can be classified into two types, the conventional model and the bend-flow model (Hsieh and Yang, 2003). The major difference between the two is the treatment of dispersion stress terms in the momentum equations. Integrating along the vertical direction of velocity from the depth-averaged values represents the dispersion stress terms. The conventional model assumes that vertical velocity is uniform while the secondary current effect is ignored. On the other hand, the bend flow model takes into account the influence of the dispersion stress terms arisen from the integration of the products of discrepancy between the mean and the adopted secondary-current velocity distribution.

Conventional models have been widely used by many researchers. Molls and Chaudhry (1995) proposed the concept of interacted effective stresses, which consists of the laminar viscosity stresses and the turbulent stresses, to simulate the experimental bend-flow data reported by Rozovskii (1961).

Ye and McCorquodal (1997) proposed a fractional two-step implicit model to simulate the experimental bend-flow data reported by Chang (1971). Ye and McCorquodal (1997) and Bui Minh Duc et al. (2004) increased the coefficient of exchange of momentum in the horizontal direction, i.e. the effective eddy viscosity, to account for the effects of the secondary motion. For the same reason, when using conventional models to simulate mass transport, it is necessary to reduce the Schmidt number to correct the dispersion effects (Jian Ye and Mc Corquodale 1997; Duan 2004). Althogh this simulation showed good agreement compared to the experiment data, conventional models are not adequate for mass transport in curved channels since the Schmidt number varies in wide range and requires calibration.

Flokestra (1977) indicate the need of dispersion stress terms for bend flow simulation. Finnie et al. (1999) later followed Flagstar's concept to solve a transport equation for streamwise vortices and incorporated the so-called associated acceleration terms, i.e., dispersion stress terms, to the depth-averaged equations. The inclusion of these acceleration terms results in improved predictions of depth-averaged velocity in bend-flow simulation. Lien et al. (1999a) further showed that the simulated results without considering the dispersion stress terms are consistent with the potential theory, in which the velocity distribution is skewed inward and away from the sidewalls and approaches to the free-vortex distribution.

Hsieh and Yang (2003) studied the suitability of 2D models for bend flow simulation by using a conventional model and a bend-flow model. The analysis of simulation results indicated that the maximum relative difference in longitudinal velocity is mainly related to the relative strength of the secondary current and the relative length of the channel. Empirical relations connecting the maximum relative difference in longitudinal velocities, the relative strength of the secondary current, and the relative length of the channel, were proposed to be used as a guideline for model users.

The purpose of this paper is to present an unsteady 2D depth-averaged flow model considering the dispersion stress terms to simulate the bend flow field. The model uses an orthogonal curvilinear coordinate system to efficiently simulate the flow field with irregular boundary. Numerically, the proposed model employes a projection and time-splitting methods for solving the flow governing equations. Two sets of experimental data measured by de Vriend and Koch (1977) and Rozovskii (1961) are used to examine the capabilities of the proposed model.

2. FLOW SIMULATION

Under the assumption of incompressible fluid, constant viscosity, and hydrostatic pressure distribution over the depth, the depth averaged equations can be obtained from integrating Navier-Stokes equation along water depth using the kinematics boundary conditions. The unsteady 2D depth-average flow governing equations including the basic continuity and momentum equations can, respectively, be written in orthogonal curvilinear (s, n) coordinates as follows:
Continuity equation:

$$\frac{\partial \xi}{\partial t}+\frac{\partial p}{\partial s}+\frac{\partial q}{\partial n}-\frac{q}{Rs}+\frac{p}{Rn}=0 \tag{1}$$

and Momentum equation
in s-direction:

$$\begin{aligned}&\frac{\partial p}{\partial t}+\frac{\partial}{\partial s}(\bar{u}p)+\frac{\partial}{\partial n}(\bar{v}p)-2\frac{pq}{hR_s}+\frac{p^2-q^2}{hR_n}+\frac{\partial D_{uu}}{\partial s}+\frac{\partial D_{uv}}{\partial n}+\tau_{bs}+gh\frac{\partial \xi}{\partial s}=\\&=\frac{\partial}{\partial s}\left(E\frac{\partial p}{\partial s}\right)+\frac{\partial}{\partial n}\left(E\frac{\partial p}{\partial n}\right)-\frac{2E}{R_s}\frac{\partial q}{\partial s}-\frac{2E}{R_n}\frac{\partial q}{\partial n}-\frac{\partial E}{\partial s}\frac{q}{R_s}-\frac{\partial E}{\partial n}\frac{q}{R_n}\end{aligned} \tag{2}$$

and in n-direction:

$$\begin{aligned}&\frac{\partial q}{\partial t}+\frac{\partial}{\partial s}(\bar{u}q)+\frac{\partial}{\partial n}(\bar{v}q)+2\frac{pq}{hR_n}+\frac{p^2-q^2}{hR_s}+\tau_{bn}+\frac{\partial D_{vv}}{\partial n}+\frac{\partial D_{uv}}{\partial s}+gh\frac{\partial \xi}{\partial n}\\&=\frac{\partial}{\partial s}\left(E\frac{\partial q}{\partial s}\right)+\frac{\partial}{\partial n}\left(E\frac{\partial q}{\partial n}\right)+\frac{2E}{R_s}\frac{\partial p}{\partial s}+\frac{2E}{R_n}\frac{\partial p}{\partial n}+\frac{\partial E}{\partial s}\frac{p}{R_s}+\frac{\partial E}{\partial n}\frac{p}{R_n}\end{aligned} \tag{3}$$

where $p=uh$ and $q=vh$ are mass fluxes in the s and n direction, respectively; τ_{bs}, τ_{bn} are the components of the bed-shear stress in the s and n direction that can be written as follows:

$$\tau_{bs}=\frac{gp\sqrt{p^2+q^2}}{C^2h^2} \tag{4}$$

$$\tau_{bn}=\frac{gq\sqrt{p^2+q^2}}{C^2h^2} \tag{5}$$

where s and n are orthogonal curvilinear coordinates in streamwise axis and transverse axis, respectively; $\bar{u}$ and $\bar{v}$ are depth-averaged velocity components in s and n direction, respectively; t is time; ξ is water surface elevation; h is flow depth; R_s and R_n are radius

of curvature of s and n axis, respectively; C is Chezy coefficient; E is eddy viscosity coefficient and D_{uu}, D_{vv}, D_{uv} are dispersion terms, their expressions are as follows

$$D_{uu} = \int_{z_b}^{z_b+h} (u-\bar{u})^2 \, dz$$

$$D_{uv} = \int_{z_b}^{z_b+h} (u-\bar{u})(v-\bar{v}) \, dz$$

$$D_{vv} = \int_{z_b}^{z_b+h} (v-\bar{v})^2 \, dz$$

where z_b bed elevation and u and v are are velocity components in the streamwise and transverse direction, respectively.

2.1. Turbulent Model

In this model, The Smagorinsky viscosity formulation with the following expression are adopted

$$E = C_s^2 \Delta^2 \sqrt{\left(\frac{\partial \bar{u}}{\partial x}\right)^2 + \left(\frac{\partial \bar{v}}{\partial y}\right)^2 + \left(\frac{\partial \bar{u}}{\partial y} + \frac{\partial \bar{v}}{\partial x}\right)^2} \tag{6}$$

Where Δ is grid spacing and C_s is a constant to be chosen in the interval of 0.25 to 1.0.

2.2. Dispersion Terms in Momentum Equations

Because of the secondary flow, the integration of his product of the discrepancy between the depth-averaged and the actual velocity can no longer be neglected. To drive the mathematical expressions of these terms. In this model, the velocity profiles in the streamwise and transverse direction proposed by de Vriend (1977) and Rozovskii (1957) are adopted, respectively

$$u = \bar{u}\left(1 + \frac{\sqrt{g}}{\kappa C} + \frac{\sqrt{g}}{\kappa C}\ln\zeta\right) = \bar{u} f_m(\zeta) \tag{7}$$

$$v = \bar{v} f_m(\zeta) + \frac{\bar{u} h}{\kappa^2 R_s}\left\{F_1(\zeta) - \frac{\sqrt{g}}{\kappa C}\left[F_2(\zeta) + 0.8\left(1+\ln\zeta\right)\right]\right\} \tag{8}$$

In which

$$f_m(\zeta) = 1 + \frac{\sqrt{g}}{\kappa C} + \frac{\sqrt{g}}{\kappa C}\ln\zeta \tag{9}$$

$$F_1(\zeta) = \int \frac{2\ln\zeta}{\zeta - 1} d\zeta \tag{10}$$

$$F_2(\zeta) = \int \frac{\ln^2\zeta}{\zeta - 1} d\zeta \tag{11}$$

Where $\zeta = \left(z - z_b\right)/h$ is dimensionless distance from the bed, z_b is bed elevation, C is Chezy Coefficient, g is gravitational acceleration and κ is Von Karman constant.

According to (7) and (8), the primary velocity profile is assumed to follow a logarithmic distribution, and the transverse velocity profiles are a combination of the secondary flow. It is obvious that only the secondary flow due to the curvature of the bend is considered in the formulation of the transverse velocity profile. Such consideration of transverse secondary flow is a main factor to shift the streamwise momentum from the inner region of a bend toward the outer region and to increase the main velocity near the outer bank. In addition, the effect of the secondary flow on the streamwise velocity profile is neglected, and these velocity profiles, used in the model, are inadequate for a reverse secondary eddy that occurred near the surface at the outer bank. Substituting Eqs. (7) and (8) into Eqs. (6) yields :

$$D_{uu}^{c} = \overline{u}^{2} h \left(\frac{\sqrt{g}}{\kappa C} \right)^{2} \tag{12}$$

$$D_{vv}^{c} = h\overline{v}^{2} \left(\frac{\sqrt{g}}{\kappa C} \right)^{2} + \frac{\overline{u}^{2} h^{3}}{\kappa^{4} R_{s}^{2}} FF_{2} + \frac{2\overline{uv} h^{2}}{\kappa^{2} R_{s}} \left(\frac{\sqrt{g}}{\kappa C} \right) FF_{1} \tag{13}$$

$$D_{uv}^{c} = h\overline{uv} \left(\frac{\sqrt{g}}{\kappa C} \right)^{2} + \frac{\overline{u}^{2} h^{2}}{\kappa^{2} R_{s}} \left(\frac{\sqrt{g}}{\kappa C} \right) FF_{1} \tag{14}$$

These dispersion terms included in equations (2) and (3) to solve for flow velocity, Where

$$FF_{1} = \int_{0}^{1} (1 + \ln \zeta) \left(F_{1}(\zeta) - \frac{\sqrt{g}}{\kappa C} F_{4}(\zeta) \right) d\zeta \tag{15}$$

$$FF_{2} = \int_{0}^{1} \left[F_{1}(\zeta) - \frac{\sqrt{g}}{\kappa C} F_{4}(\zeta) \right]^{2} d\zeta \tag{16}$$

Where $F_{4}(\zeta) = \left(F_{2}(\zeta) + 0.8\left(1 + \ln \zeta\right) \right)$. Note that equations (15) and (16) can be integrated numerically using the trapezoidal rule.

3. NUMERICAL ALGORITHM

The present model used finite volume projection method approach for solving the governing equation in a staggered grid. The key feature of this method is to solve governing equation in three steps. The first step is to compute the mass fluxes (*p* and *q*) in the momentum equations without considering the pressure terms and continuity equation. The second step is to compute the water elevation with implicit scheme in two stages. The first stage is to compute the water elevation in time step *t*+1/2 by solving continuity equation and pressure term equation (17) that remaining from momentum equations in *s* direction where time step *t*+1/2 denotes the intermediate step between *t* and *t*+1. The second stage of second step is to compute water elevation in time step *t*+1 by solving continuity equation and pressure term equation (18) that remaining from momentum equations in *n* direction.

$$\frac{\partial p}{\partial t} + gh \frac{\partial \xi}{\partial s} = 0.0 \tag{17}$$

$$\frac{\partial q}{\partial t} + gh \frac{\partial \xi}{\partial n} = 0.0 \tag{18}$$

The last step is to modify the provisional mass fluxes using water elevation value and equations (17) and (18). They are expressed sequentially as follows:

First step:

$$\frac{p_{j,k}^{t+1/2}-p_{j,k}^{t}}{\Delta t}+\frac{(\overline{up})_{j-1/2,k}^{t}-(\overline{up})_{j+1/2,k}^{t}}{\Delta s_{j,k}}+\frac{(\overline{vp})_{j,k+1/2}^{t}-(\overline{vp})_{j,k-1/2}^{t}}{\Delta n_{j,k}}-2(\frac{q}{hR_s})_{j,k}^{t}p_{j,k}^{t+1}+$$

$$\frac{p_{j,k}^{t+1/2}p_{j,k}^{t}-(q_{j,k}^{t})^2}{(hR_n)_{j,k}^{t}}+\frac{(D_{uu}^{c})_{j+1/2,k}^{t}-(D_{uu}^{c})_{j-1/2,k}^{t}}{\Delta s_{j,k}}+\frac{(D_{uv}^{c})_{j,k+1/2}^{t}-(D_{uv}^{c})_{j,k-1/2}^{t}}{\Delta n_{j,k}}+$$

$$(\frac{gn_m^2\sqrt{p^2+q^2}}{h^{7/3}})_{j,k}^{t}p_{j,k}^{t+1/2}=\frac{\left(E\frac{\partial p}{\partial s}\right)_{j+1/2,k}^{t}-\left(E\frac{\partial p}{\partial s}\right)_{j-1/2,k}^{t}}{\Delta s_{j,k}}+\frac{\left(E\frac{\partial p}{\partial n}\right)_{j,k+1/2}^{t}-\left(E\frac{\partial p}{\partial n}\right)_{j,k-1/2}^{t}}{\Delta n_{j,k}}-$$

$$(\frac{2E}{R_s})_{j,k}^{t}\frac{q_{j+1/2,k}^{t}-q_{j-1/2,k}^{t}}{\Delta s_{j,k}}-(\frac{2E}{R_n})_{j,k}\frac{q_{j,k+1/2}^{t}-q_{j,k-1/2}^{t}}{\Delta n_{j,k}}-(\frac{q}{R_s})_{j,k}^{t}\frac{E_{j+1/2,k}^{t}-E_{j-1/2,k}^{t}}{\Delta s_{j,k}}-$$

$$(\frac{q}{R_n})_{j,k}^{t}\frac{E_{j,k+1/2}^{t}-E_{j,k-1/2}^{t}}{\Delta n_{j,k}} \qquad (19)$$

Similarly, the difference form of mass flux component in *n* direction can be derived from equation (3). Superscript *t* denotes the known variables at time step *t*, and superscript *t*+1 denotes the unknown variables at time step *t*+1. Subscript *j, k* denotes the variables position in *s* and *n* direction, respectively in computational domain.

The first step includes convection and diffusion terms companied with additional terms in the momentum equations due to the curving grid line and dispersion terms. This model used time-splitting method for solving momentum equations terms. In this method it has been assumed that the influence of different processes might best be computed separately as several stages in a several different scheme. It is important to note that in the next stage the input for computations is taken from the first process and not from the actual preceding time level. In the first step, advection and diffusion terms in momentum equations are solved using the second order explicit from and implicit schemes, respectively. Other terms in these equations are solved using implicit scheme. In the next step, mass fluxes $p^{t+1/2}, q^{t+1/2}$ are computed using equations (21) and (22).

3.1. Second step, First stage

Continuity

$$\frac{\xi_{j,k}^{t+1/2}-\xi_{j,k}^{t}}{0.5\Delta t}+\frac{(p_{j+1/2,k}^{t+1}-p_{j-1/2,k}^{t+1})}{\Delta s_{j,k}}+\frac{(q_{j,k+1/2}^{t}-q_{j,k-1/2}^{t})}{\Delta n_{j,k}}-\frac{q_{j,k}^{t}}{Rs_{j,k}}+\frac{p_{j,k}^{t+1}}{Rn_{j,k}}=0 \qquad (20)$$

Using equation (17)

$$p_{j+1/2,k}^{t+1}=[p_{j+1/2,k}^{t+1/2}-gh_{j+1/2,k}^{t}\frac{\Delta t}{\Delta s_{j,k}}(\xi_{j+1,k}^{t+1/2}-\xi_{j,k}^{t+1/2})] \qquad (21)$$

$$p_{j-1/2,k}^{t+1}=[p_{j-1/2,k}^{t+1/2}-gh_{j-1/2,k}^{t}\frac{\Delta t}{\Delta s_{j,k}}(\xi_{j,k}^{t+1/2}-\xi_{j-1,k}^{t+1/2})] \qquad (22)$$

Water elevation in time step *t*+1/2 i.e. $\xi^{t+1/2}$ computed with substituting equations (21) and (22) into equation (20).

3.2. Second step, Second stage

Continuity

$$\frac{\xi_{j,k}^{t+1}-\xi_{j,k}^{t+1/2}}{0.5\Delta t}+\frac{(p_{j+1/2,k}^{t}-p_{j-1/2,k}^{t})}{\Delta s_{j,k}}+\frac{(q_{j,k+1/2}^{t+1}-q_{j,k-1/2}^{t+1})}{\Delta n_{j,k}}-\frac{q_{j,k}^{t+1}}{Rs_{j,k}}+\frac{p_{j,k}^{t}}{Rn_{j,k}}=0 \quad (23)$$

using equation (18)

$$q_{j,k+1/2}^{t+1}=[q_{j,k+1/2}^{t+1/2}-gh_{j,k+1/2}^{t}\frac{\Delta t}{\Delta n_{j,k}}(\xi_{j,k+1}^{n+1}-\xi_{j,k}^{n+1})] \quad (24)$$

$$q_{j,k-1/2}^{t+1}=[q_{j,k-1/2}^{t+1/2}-gh_{j,k-1/2}^{t}\frac{\Delta t}{\Delta n_{j,k}}(\xi_{j,k}^{t+1}-\xi_{j,k-1}^{t+1})] \quad (25)$$

Water elevation in time step $t+1$, ξ^{t+1} is computed with substituting equations (24) and (25) into equation (23).

3.3. Last step

Using equations (21),(22) and equations (24),(25) through water elevation in time step $t+1$ mass fluxes p and q in time step $n+1$ are computed.

3.4. Boundary Condition

Three types of boundaries, namely, the inlet or upstream end, outlet or downstream end, and solid walls are considered. Discharge hydrograph per unit width can be specified at the inlet section. Water surface elevation can be specified at the outlet section. At the solid boundaries the flow velocity is assumed to be zero.

4. RESULTS

4.1. Model Verifications

To test and verify the performance and the capabilities of the proposed model two sets of experimental data on bend flow conducted by de Vriend (1979) and Rozovskii (1961) are adopted. These selected channels belong to mildly curved and sharply curved channels, respectively. Data regarding the channel dimensions and flow conditions are summarized in Table 1.

4.2. Flow in a mildly curved channel

In de Vriend (1979) experiment, the channel consists of a 1.7 m wide flume having a U-shaped plan. With a horizontal bottom and vertical sidewalls, the radius of curvature of the flume axis in the bend is 4.25 m and the upstream and downstream straight reaches have an effective length of about 6.0 m. The ratio of radius of curvature to channel width is 3.5. The discharge at the inlet is 0.0671 m^3/s. The averaged velocity is 0.202 m/s, and the averaged flow depth is 0.1953 m.

"Figure 1(a)" shows the velocity redistribution across the channel width along the bend without considering the dispersion stresses. The simulated results are consistent with the potential theory by which the velocity is inversely proportional to the radius of the curvature. Hence, the flow velocity along the channel bend is higher in the inner bank region than that in the outer bank region, as clearly shown in "figure 1(a)" while the flow velocity at the inner and outer banks are almost equal at the inlet of the bend.

Table1. Channel geometry and flow parameters of simulated cases

Case	Discharge Q (m^3/s)	Width B (m)	Depth d (m)	Velocity V (m/s)	R/B
De Vriend (1979)	0.0671	1.7	0.1953	0.202	3.5
Rozovskii (1961)	0.0123	0.8	0.053	0.265	1.0

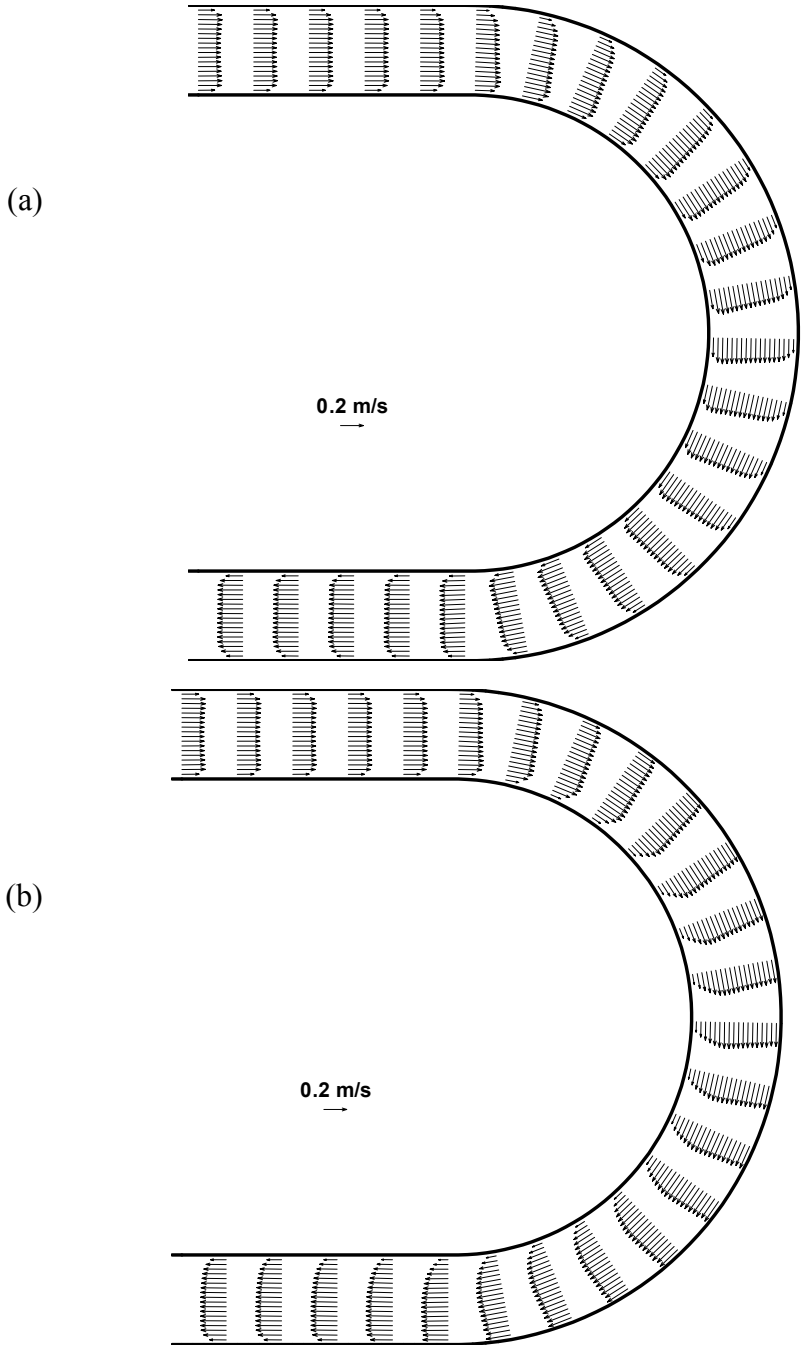

Figure 1 Velocity redistribution by numerical simulation for mildly curve: (a) ignoring secondary flow; (b) taking secondary flow into account

If the dispersion stresses are included in the bend flow simulation, they act as sink or source in the momentum equation, which cause the transverse convection of momentum to shift from the inner bank to the outer bank (Kalkwijk and de Vriend 1980; de Vriend

1981). "Figure 1(b)" shows the simulated results with dispersion stress, which clearly demonstrate a shift of the maximum main velocity along the channel bend from the inner-bank region toward the outer bank region. However, for this mild bend, the radius of channel curvature is much larger than the width of the channel and thus the effect of secondary flow is very weak.

The comparison of simulated water surface elevation with the measurement at the inner bank and outer bank for the cases with or without the dispersion terms is plotted in "figure 2".

It shows that water surface elevation at the outer bank is at much higher level than that in the inner bank throughout the bend. The rise of flow at the outer bank results from the centrifugal force. One also can discern a little difference between the result with and without the dispersion terms. In general, the simulated water elevations are in agreement with the measurement at the inner and outer banks, separately. The difference between the simulated results with and without secondary flow is not significant because the secondary flow effect in mild bend is weak.

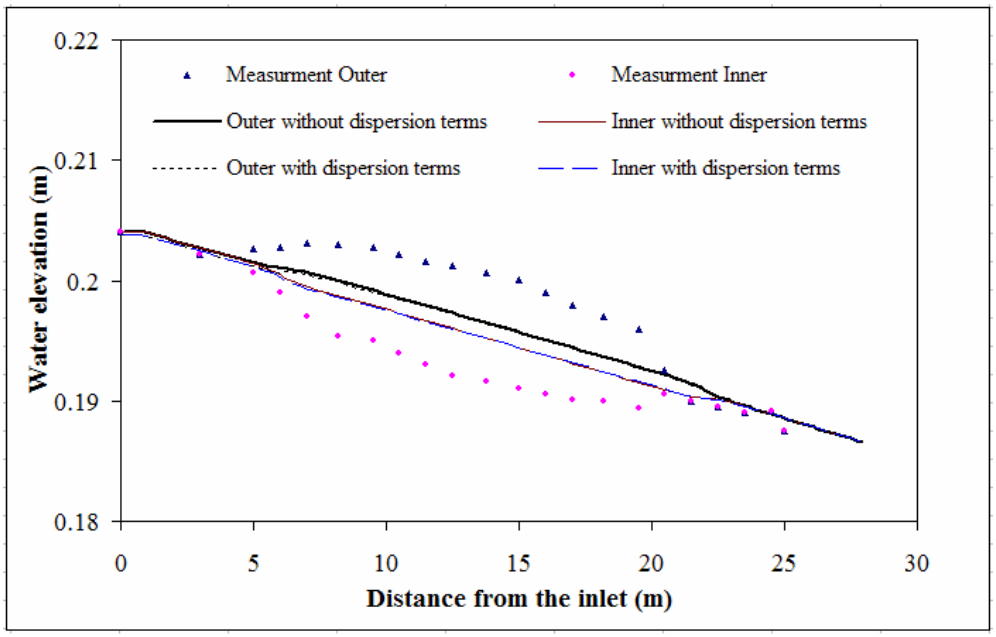

Figure 2 Comparison between sidewall flow depth with and without secondary flow; mildly curved

4.3. Flow in a sharply curved channel

The present 2D model was also applied to the experimental results obtained by Rozovskii (1961) in a sharply curved flume. The flume includes a 180 curved reach with a 6 m long straight approach and a 3 m long straight exit. The ratio of mean radius of curvature to width is 1.0. The width of the channel is 0.8 m. The cross section of the bend is rectangular and connected to the straight inlet and outlet reaches of the same cross section. Water depth at the downstream end is 0.053 m, and the discharge is 0.0123 m/s.

"Figure 3(a)" and "3(b)" show the computed velocity distribution across the channel width with and without secondary flow effects, respectively. As shown in figure 3(a), the velocity at the inner bank becomes larger while that at the outer bank becomes smaller when the flow enters the bend. Such a flow pattern prevails through the entire bend. The simulated velocity distribution becomes relatively uniform after a distance downstream of the bend exit. When considering the secondary flow effect, "figure 3(b)" indicates different velocity distributions after the flow enters the bend. In this situation the

maximum main velocity along the channel bend shift of from the inner bank region toward the outer bank region.

"Figure 3(b)" shows that the velocity distribution with the secondary flow effect is no longer uniform in the straight cannel even after the flow exits the bend. The velocity near the outer bank region abruptly speeds up, and the corresponding velocity near the inner-bank region decelerates. This phenomenon can be explained by the decline of the transverse slope of the water surface and the release of the remaining additional momentum by the secondary flow effect when the radius of curvature at the bend exit abruptly changes to infinity.

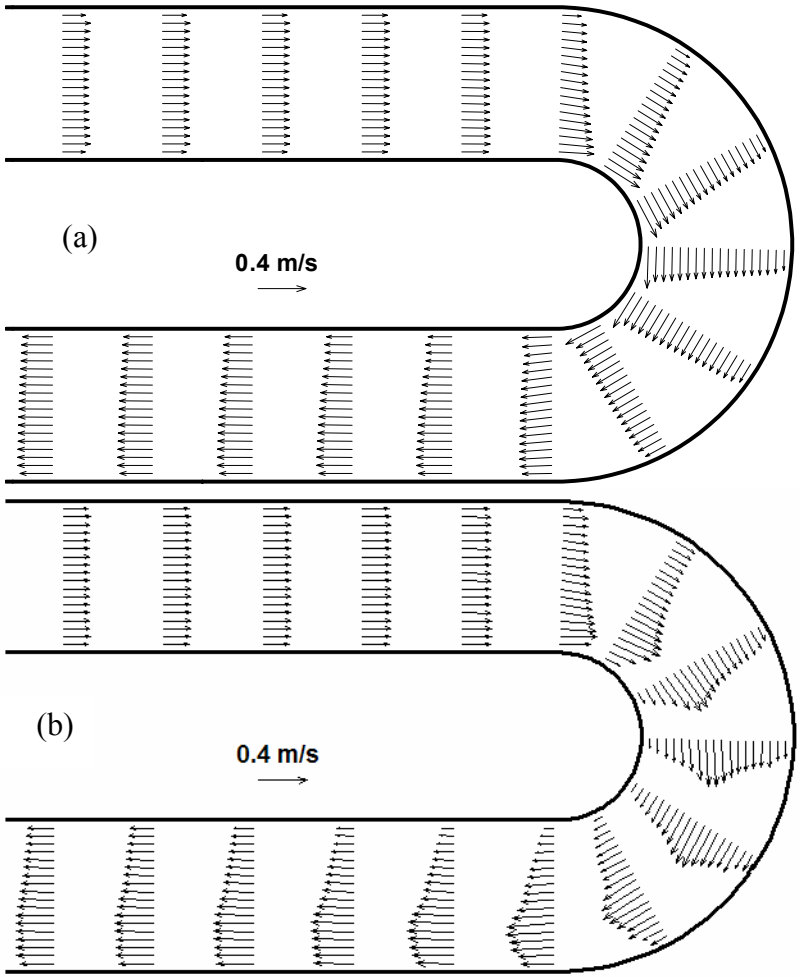

Figure 3 Velocity redistribution by numerical simulation for sharp curve, (a) without secondary flow, (b) with secondary flow

"Figure 4" shows the comparison of simulated surface elevation with and without the dispersion terms along the channel length. It can be seen that, along the bend, the water level rises at the outer bank and falls at the inner bank. Note that, without the secondary flow effect, the water level will be underestimated at the outer bank. Furthermore, the consideration of the secondary flow effect and decrease the slope of super elevation between the inner bank and outer bank as observed in measured data.

This result showed that the impact of secondary flow on the depth-averaged flow distribution and water surface elevations becomes more visible with increasing channel curvature.

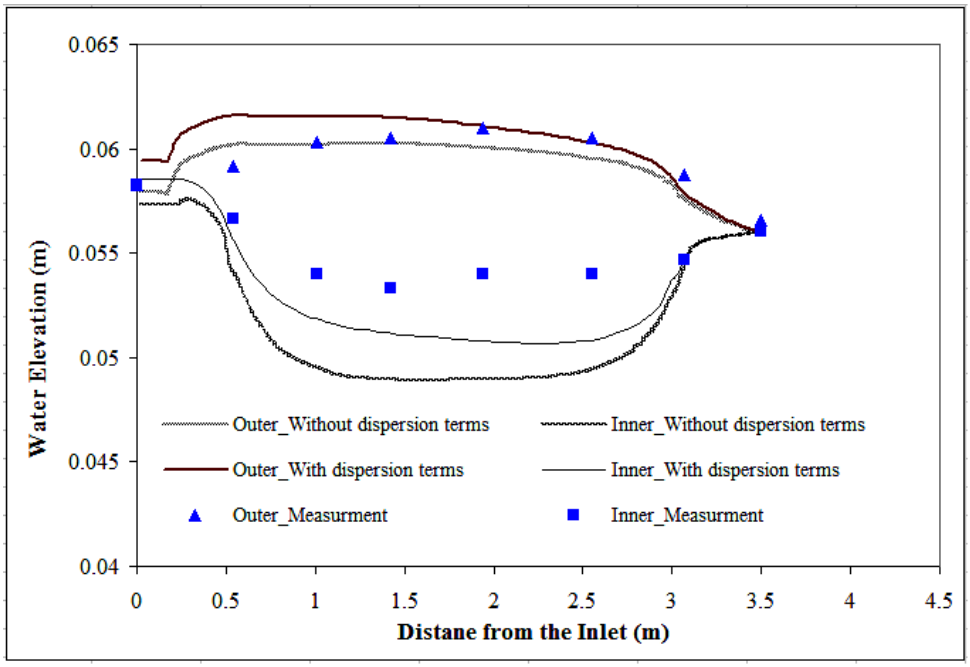

Figure 4 comparison between sidewall flow depth with and without secondary flow; sharply curved

5. DISCUSSION

This paper presents an unsteady 2D depth averaged model developed using orthogonal curvilinear coordinate system. The model takes into account vertical velocity profiles in a bend using them to capture the effect of dispersion stress on the floor. Dispersion stress terms serve as a sink or source in the momentum conservation equations are needed to calculate the transverse convection of momentum caused by the secondary flow along a channel bend (Kalkwijk and de Vriend 1980; de Vriend 1981). If the dispersion stress terms are neglected, the government equations reduce to a conventional depth averaged equation assuming uniform velocity over depth. In other words, the model presented herein should be more applicable for practical application in bend flow modeling than the conventional depth averaged models because of its ability to account for the secondary flow effect.

Two sets of experimental bend-flow data, one with mild bends and one with sharp bends, were used to demonstrate the capabilities of the proposed model. The simulated water elevation results and experimental data agree well in both cases of the mildly and sharp curved channel, the computed results show that the secondary flow effect has been properly represented by calculating the dispersion stresses. In short, the dispersion stresses play an important role in accurately simulating or predicting flow fields in sharp bends as well as in mild bends.

ACKNOWLEDGMENTS

This study is part of the Ph.D thesis of first writer in Tarbiat Modares university of Iran, department of agriculture.

REFERENCES

Bui Minh Duc, et al. (2004), Numerical modeling of bed deformation in laboratory channels, *Journal of hydraulic Engineering*, ASCE, 130(9), pp.894-904.

de Vriend, H. J. (1977), A mathematical model of steady flow in curved shallow channel, *Hydr. Res*., Delft, The Netherlands, 15(1), pp. 37-54.

de Vriend, H. (1979), Flow measurement in a curved rectangular channel, *Internal Report, No. 9-97. Tech. Rep.*, Laboratory of Fluid Mechanics, Depth. Of Civil Engineering, Delft Univ. of Technology, Delft, The Netherlands.

de Vriend. H. (1980), Velocity redistribution in curved rectangular channels. Journal of fluid mechanics., 107, 423-439.

de Vriend. H. (1981), Flow measurement in a curved rectangular channel. Part 2: Rough bottom. Internal Report, No. 5-81. Tech. Rep., Laboratory of Fluid Mechanics, Depth. Of Civil Engineering, Delft Univ of technology, Delft, The Netherlands.

Darby, S. E., Alabyan, A. M., and Van De Weil, M. J. (2002), Numerical simulation of bank erosion and channel migration in meandering rivers, *Water Resource Research*, 38(9), 2-1-12.

Flokestra, C. (1977), The closure problem for depth averaged two dimensional flows, *Proc. 18th Congress of the int*. Association for hydraulic research, pp. 247-256.

Fnnie et al. (1999), Secondary flow correction for depth averaged flow calculation, *Journal of hydraulic mechanics*, 125(7), pp. 848-858.

Howard, A. (1984), Simulation model of meandering, *River meandering*, C. Elliot, ed., ASCE, New York, pp. 952-963.

Jennifer G. Duan (2004), Simulation of flow and mass dispersion in meandering channels, *Journal of hydraulic Engineering* , ASCE, 130(10), pp. 964-976.

Johannesson, H., and parker, G. (1989a), Secondary flow in a mildly sinuous channel, *Journal of Haydraulic Engineering*, 115(3), pp. 289-308.

Johannesson, H., and parker, G. (1989b), Velocity redistribution in meandering rivers, *Journal of Haydraulic Engineering*, 115(8), pp. 1019-1039.

Leschziner, M. A., and Rodi, W. (1979), Calculation of strongly curved open channel flow, *Journal of hydraulic division*, ASCE, 105(10), pp. 1297-1314.

Lien, H. C., Hsieh, T. Y., and Yang, J. C. (1999), Use of two-step split operator approach for 2D shallow water flow computation. *Int. Journal methods in fluids*

Mockmore, C. (1943), Flow around bends in stable channels, *Trans.,* ASCE, 3, 334.

Molls, T., and Chaudhry, M. H. (1995), Depth-averaged open-channel flow model, *Journal of hydraulic Engineering*, 121(6), pp. 453-465.

Nelson, J., and Smith, J. (1989), Evolution and stability of erodible channel beds, *Technical report*, American Geophysics Union, Washington, D.C.

Odgaard, A. j. (1989), River meander model. I: Development, *Journal of hydraulic Engineering*, ASCE, 115(11), pp. 1433_1450.

Rozovskii, I. L. (1961), Flow of water in bends of open channels. *The Israel program for scientific Translations*, Jerusalem.

Sinha, S. K., Sotiropoulos, F., and Odgaard, A. J. (1998), Three dimensional numerical model for flow through natural rivers, *Journal of hydraulic Engineering* , ASCE, 124(1), pp. 13-24.

Shukhry, A. (1949), Flow around bends in an open flume. *Journal of Hydraulic Divission*, ASCE, 75,713.

Shimizu, Y., Yamaguchi, H., and Itakura, T. (1990), Three dimensional computations of flow and bed deformation, *Journal of hydraulic Engineering*, ASCE, 116(9), pp. 1090-1108.

Smith, J. (1984), A model for flow in meandering streams, *Water Resource Research*, 20(9), pp. 1301-1315.

T. Y. Hsieh and J. C. Yang (2003), Investigation on the suitability of two dimensional depth averaged models for bend flow simulation, *Journal of Hydraulic Engineering*, ASCE, 129(8), pp. 597-612.

Ye, J., and McCorquodale, J. A. (1997), Depth averaged hydrodynamic model in curvilinear collocated grid, *Journal of Hydraulic Engineering*, 123(5), pp. 380-388.
Yen, B. C. (1965), Characteristics of subcritical flow in a meandering channel, *PhD thesis*, University of Iowa, Iowa City, Iowa.
Yeh, K. C., and Kennedy, J. F. (1993a), Moment model of nonuniform channel bend flow. I: Fixed beds, *Journal of Hydraulic Engineering*, ASCE, 119(7), pp. 776-795.
Yeh, K. C., and Kennedy, J. F. (1993b), Moment model of nonuniform channel bend flow. II: Erodible beds, *Journal of Hydraulic Engineering*, ASCE, 119(7), pp. 796-815.